LETTERS

Unusual magnetic order in the pseudogap region of the superconductor $HgBa_2CuO_{4+\delta}$

Y. Li[1], V. Balédent[2], N. Barišić[3,4], Y. Cho[3,5], B. Fauqué[2], Y. Sidis[2], G. Yu[1], X. Zhao[3,6], P. Bourges[2] & M. Greven[3,7]

The pseudogap region of the phase diagram is an important unsolved puzzle in the field of high-transition-temperature (high-T_c) superconductivity, characterized by anomalous physical properties[1,2]. There are open questions about the number of distinct phases and the possible presence of a quantum-critical point underneath the superconducting dome[3–5]. The picture has remained unclear because there has not been conclusive evidence for a new type of order. Neutron scattering measurements for $YBa_2Cu_3O_{6+\delta}$ (YBCO) resulted in contradictory claims of no[6,7] and weak[8,9] magnetic order, and the interpretation of muon spin relaxation measurements on YBCO[10,11] and of circularly polarized photoemission experiments on $Bi_2Sr_2CaCu_2O_{8+\delta}$(refs 12, 13) has been controversial. Here we use polarized neutron diffraction to demonstrate for the model superconductor $HgBa_2CuO_{4+\delta}$ (Hg1201) that the characteristic temperature T^* marks the onset of an unusual magnetic order. Together with recent results for YBCO[14,15], this observation constitutes a demonstration of the universal existence of such a state. The findings appear to rule out theories that regard T^* as a crossover temperature[16–18] rather than a phase transition temperature[19–21]. Instead, they are consistent with a variant of previously proposed charge-current-loop order[19,20] that involves apical oxygen orbitals[22], and with the notion that many of the unusual properties arise from the presence of a quantum-critical point[3–5,19].

YBCO has a relatively complicated orthorhombically distorted crystal structure, with two CuO_2 layers forming a double layer in the unit cell and with additional Cu–O chains between the double layers. Recent experiments[14,15] on YBCO point to the possible existence of a new magnetic order below T^* (see Fig. 1a) that does not break translational invariance. The observed effect occurs at positions in reciprocal space that had not been considered in previous work. To assess whether this effect is unique to YBCO or a universal property of the high-T_c superconductors, it is essential to extend the investigation to additional, structurally simpler compounds. Hg1201 has a simple tetragonal crystal structure (Fig. 1e), with only one CuO_2 layer in the unit cell, and the highest maximum T_c of all known single-layer compounds[23,24]. These properties, together with a wide accessible doping range and minimal effects of disorder[24,25], render Hg1201 an ideal system for the clarification of the pseudogap physics. Through recent advances in crystal growth, sizable high-quality single crystals have finally become available[26], making the present study possible.

Polarized neutron diffraction experiments were made on the 4F1 triple-axis spectrometer at the Laboratoire Léon Brillouin. The experimental setup was similar to that described previously[14], allowing the detection of scattered neutrons in both spin-flip (SF) and non-spin-flip (NSF) channels. We define the flipping ratio $FR = I_{NSF}/I_{SF}$ (where I is intensity) to quantify the experimental efficiency of polarization. With careful arrangement, a stable flipping ratio as high as 95 can be obtained. This proved to be crucial for the detection of small magnetic signals in samples with relatively high carrier concentration. All measurements were performed in the $(H0L)$ scattering plane, where the scattering wave vector is quoted as $\mathbf{Q} = H\mathbf{a}^* + K\mathbf{b}^* + L\mathbf{c}^* \equiv (HKL)$ in units of the reciprocal lattice vectors, with typical room temperature values $a^* = b^* = 1.614\,\text{Å}^{-1}$ and $c^* = 0.657\,\text{Å}^{-1}$. Four underdoped samples were investigated; as revealed in Fig. 1b, they show sharp superconducting transitions with $T_c = 61$, 79, 81 and 89 K.

Figure 2a–c demonstrates the existence of a magnetic component in the spin-flip channel for samples A and B. Because of the relatively strong intensity from unavoidable nuclear Bragg peak leakage in the spin-flip geometry, the measurement was made at the weak nuclear reflection $\mathbf{Q} = (101)$. The neutron polarization was parallel to the momentum transfer, $\mathbf{P}//\mathbf{Q}$, a geometry in which all magnetic scattering occurs in the spin-flip channel. The linear slope of the nuclear scattering observed in the non-spin-flip channel can be accounted for by the Debye–Waller factor. As expected, owing to the leakage, the spin-flip data have a linear nuclear scattering contribution as well. However, the spin-flip data also show an additional component below $T_{mag} \approx 250$ K, which we conclude to be of magnetic origin (see also below). The two samples have nearly identical values of T_c and T_{mag}, and the strength of the magnetic signal is nearly indistinguishable after normalization by the nuclear scattering intensity (Fig. 2b,c). The onset of magnetic order in YBCO has been associated with the pseudogap temperature T^*_ρ determined by resistivity measurements[14]. Resistivity data for a separate small crystal with $T_c = 79$ K are shown in Fig. 1c. Indeed, the rescaled magnetic intensities for samples A and B follow the deviation from linear resistivity quite well (Fig. 1d), strongly suggesting that the observed magnetic and charge properties share the same physical origin.

For new magnetic order associated with the pseudogap phase, it is expected that the ordering temperature and strength increase (decrease) towards lower (higher) doping. To test this, we subjected sample B to a reducing heat treatment that lowered the oxygen (and, consequently, the hole carrier) concentration. The resultant sample B′ has a significantly lower T_c of 61 K. Indeed, as displayed in Fig. 2e,f, the onset of the magnetic order has shifted to significantly higher temperature, and the signal strength has increased by more than a factor of five. On the other hand, for the most highly doped crystal (sample C; $T_c = 89$ K), we were no longer able to discern a magnetic signal within the counting statistics of the experiment (Fig. 2d).

Comparison between Hg1201 and YBCO[14,15] demonstrates remarkable universality (Fig. 3). (i) In both cases, the order preserves the translational symmetry of the underlying lattice, unlike conventional

[1]Department of Physics, Stanford University, Stanford, California 94305, USA. [2]Laboratoire Léon Brillouin, CEA-CNRS, CEA-Saclay, 91191 Gif sur Yvette, France. [3]Stanford Synchrotron Radiation Laboratory, Stanford, California 94309, USA. [4]1. Physikalisches Institut, Universität Stuttgart, Pfaffenwaldring 57, 70550 Stuttgart, Germany. [5]BK21 Team of Nano Fusion Technology, Pusan National University, Busan 609-735, Korea. [6]State Key Lab of Inorganic Synthesis and Preparative Chemistry, College of Chemistry, Jilin University, 2699 Qianjin Street, Changchun 130012, China. [7]Department of Applied Physics, Stanford University, Stanford, California 94305, USA.

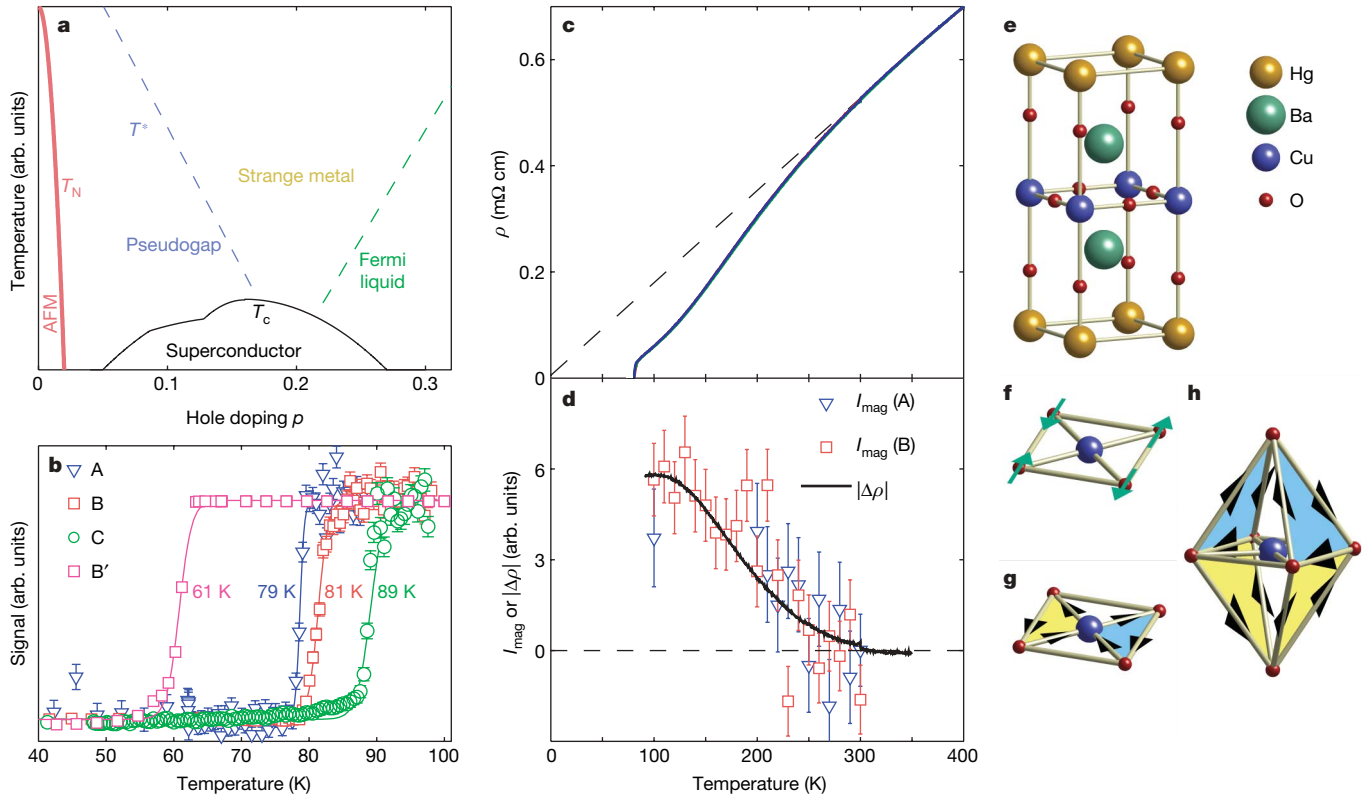

Figure 1 | Pseudogap in underdoped Hg1201. a, Schematic phase diagram of hole-doped high-T_c superconductors. T_N, Néel temperature of antiferromagnetism (AFM). **b**, Determination of T_c by superconducting quantum interference device (SQUID) magnetometry (for B′) and neutron depolarization (for A, B, C) of the four underdoped Hg1201 samples studied in this work. Quoted T_c values are transition mid-points. Sample B′ was obtained from sample B (mass ~600 mg, as-grown) by annealing in partial vacuum (0.1 torr) at 450 °C. Samples A (150 mg) and C (1.2 g) are as-grown. Typical sample mosaic is less than 0.5° (full width at half maximum). The neutron-depolarization effect was used to measure the bulk T_c whenever possible. A guide field of ~10 Oe was applied along the beam path. After the samples were cooled below T_c and contained trapped vortices, the guide field at the sample position was turned by 90°, resulting in an abrupt change of magnetic field at the sample surface, which can be observed as a decrease in flipping ratio. Error bars represent counting statistics (one standard deviation). In several cases, T_c was verified using conventional magnetic susceptibility measurements. **c**, Temperature dependence of resistivity for a separate crystal (T_c = 79 K). The resistivity measurement used the standard four-probe method, with electrical contacts sputtered on the *ac*/*bc* faces of a small single crystal (contact resistance less than 1 ohm). **d**, Deviation from linear resistivity compared with magnetic signal intensity (I_{mag}) for samples A and B, demonstrating that the new form of magnetic order is linked to the pseudogap. Error bars represent counting statistics (one standard deviation). **e**, Crystal structure of Hg1201 (dopant oxygen atoms in Hg–O layer not shown). **f–h**, Simplified schematic illustrations of three ordered states that break time-reversal symmetry, but preserve translational symmetry: **f**, spin-order involving oxygen atoms; **g**, planar orbital currents; **h**, orbital currents involving apical oxygens.

(½, ½,0) type antiferromagnetism. (ii) The magnetic scattering develops below a temperature which coincides with T^* determined from d.c. transport, suggesting that the order involves both magnetic and charge degrees of freedom. (iii) The magnetic signal is of comparable strength for the two compounds, it is strongest in very underdoped samples, and the transition appears to be continuous. We note that the effect in the most underdoped sample B′ is very strong, corresponding to ~$0.2\mu_B$ per unit cell in a naïve picture of spin-based moments, and that the present data statistics do not allow a reliable determination of the order parameter critical exponent. (iv) Using previous estimates[27,28] for the doping dependence of T_c, the ordering temperatures for both systems fall onto the same line. Linear extrapolation suggests that T_{mag} approaches zero close to the value $p_c = 0.19$, which has been argued to be the location of a quantum critical point[5]. Alternatively, rescaling $T_c(p)$ for Hg1201 to the curve for YBCO shifts $T_{mag}(p)$ to higher hole concentrations and leads to an apparent disappearance of the magnetic signal near $p = 0.15$ for both systems (Supplementary Fig. 1). Both the linear trend and the value of p_c are consistent with new polar Kerr effect results for YBCO that also indicate the existence of a phase with broken time-reversal symmetry, although with ordering temperatures that are systematically lower[29]. (v) In both cases, the moment does not lie along the *c* axis, but rather has a considerable in-plane component. For sample B, the (101) intensity measured with $\mathbf{P} \perp \mathbf{Q}$ ($\mathbf{P}$ in the scattering plane) is about 65% of that for $\mathbf{P}//\mathbf{Q}$ (Fig. 2c). Noting that polarized neutron diffraction in the spin-flip channel probes the component of the magnetic moments perpendicular to both $\mathbf{P}$ and $\mathbf{Q}$, and that in the former geometry $\mathbf{P}$ makes a relatively small angle with the *c* axis, this suggests a non-negligible component of the measured moment in the *a*–*b* plane.

The observation of magnetic Bragg scattering at $\mathbf{Q} = (101)$ is consistent with an even number of moments per unit cell with zero net moment. Magnetic order involving spin moments on the planar oxygen atoms (Fig. 1f) could, in principle, preserve the translational invariance of the underlying crystal lattice[14]. However, such order would be difficult to reconcile with the unusual moment direction and, as discussed below, with the observed strong *Q*-dependence. Moreover, it should be discernable with NMR, yet no such evidence has been reported[25]. Instead, it seems likely that the new state arises from circulating charge currents[19,20]. The experiments for Hg1201 and YBCO[14,15] are qualitatively consistent with magnetism due to two counter-circulating charge current loops per CuO_2 plaquette (Fig. 1g), but as the theory involves the planar oxygen *p* and copper *d* orbitals, it predicts a magnetic moment along the *c* axis, which cannot explain the in-plane component found experimentally. To explain the unusual moment direction and the tiny ferromagnetic component observed by the polar Kerr effect[29], it has been proposed that the relatively low structural symmetry of YBCO will lead to spin–orbit coupling that causes spin order to accompany planar loop-current

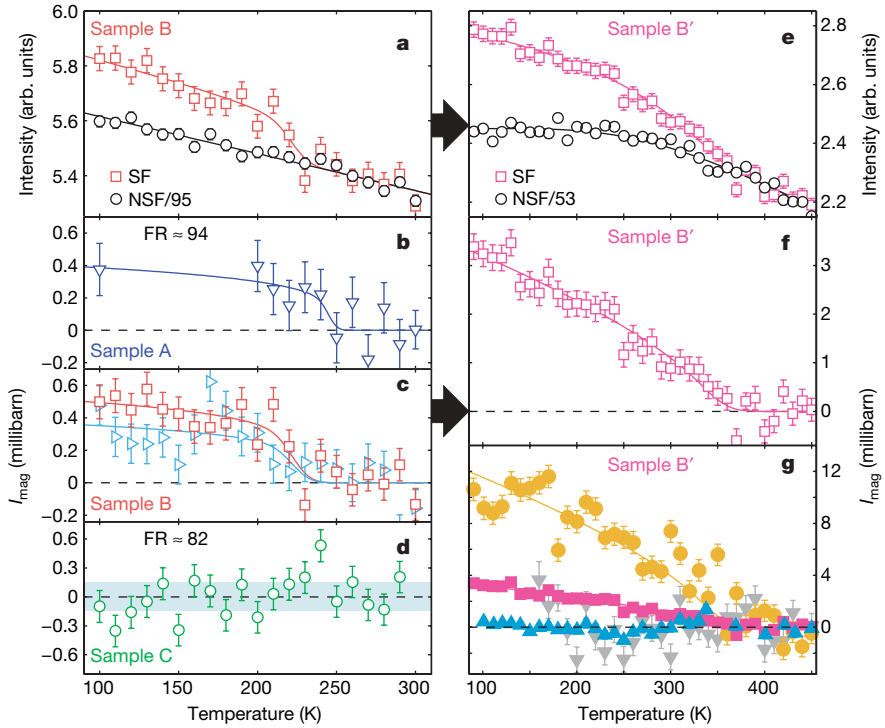

Figure 2 | Unusual magnetic order revealed by polarized-neutron diffraction. **a**, **e**, Raw data for samples B ($T_c = 81$ K) and B′ ($T_c = 61$ K). Magnetic signal appears as additional intensity in the spin-flip (SF) channel compared with 'background' intensity due to nuclear Bragg scattering. The latter is measured in the non-spin-flip (NSF) channel, but a fraction 1/FR (where FR is the flipping ratio, such as 95 in 'NSF/95') is also observed in the spin-flip geometry. **b–d**, **f**, Temperature dependence of net intensity I_{mag}, which is obtained after the removal of the background. Sample A, $T_c = 79$ K; sample B, $T_c = 81$ K; sample C, $T_c = 89$ K. Conversion to absolute units is completed using the intensity of the same nuclear Bragg peak. **g**, Intensity measured on different Bragg peaks in the most underdoped sample. Yellow circles, (100); red squares, (101); blue triangles, (201); grey inverted triangles, (102). Data in **a–f** are collected on the Bragg peak **Q** = (101), with the neutron spin parallel to **Q**. In **c**, data are also collected with the neutron spin perpendicular to **Q** in the scattering plane (red squares, **P**//**Q**; blue triangles, **P** ⊥ **Q**). Horizontal band in **d** represents an upper bound estimate for the intensity of sample C. Solid coloured lines in **a–c** and **e–g** are guides to the eye. Horizontal arrows represent the oxygen-anneal step carried out to obtain sample B′. Error bars represent counting statistics (one standard deviation). The polarized-neutron diffraction experiment was carried out in continuous runs with minimal instrument movement. The super-mirror polarizer and Heusler analyser were arranged such that the electromagnetic spin flipper was off when measuring the spin-flip channel, providing maximum stability. The experiments are limited to temperatures above T_c, because the required neutron guide field cannot be reliably sustained in the superconducting state.

order[30]. However, such spin–orbit coupling is expected to be absent in Hg1201, which possesses a high tetragonal structural symmetry in which the planar Cu and O sites are centres of inversion. The presence of significant oxygen spin moments is furthermore inconsistent with the narrow ^{17}O NMR linewidth[25].

The correct description might be a variant of the proposed phase, with orbital-current loops that involve the apical oxygens, but without current flow through the copper site (Fig. 1h). The tilt angle spanned by the CuO_2 plane and the 'oxygen triangles' is about 64° for Hg1201 and 59° for YBCO, consistent with the fact that a large portion of the total signal (**P**//**Q**) is distributed in the **P** ⊥ **Q** geometry

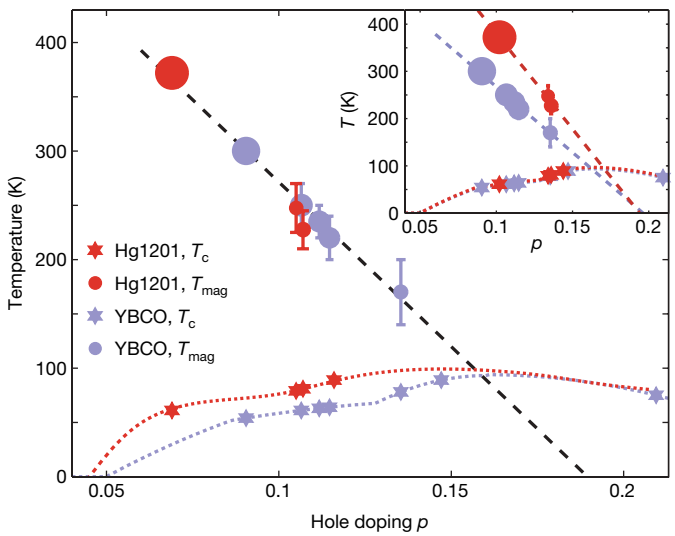

Figure 3 | Universal pseudogap phase diagram. In the main panel, hole doping is estimated from the $T_c(p)$ relationships (dotted lines) reported in[27,28]. Values of T_{mag} for Hg1201 and YBCO are determined in this work and in refs 14,15, respectively. A linear fit of $T_{mag}(p)$ to the combined data extrapolates to $T_{mag} = 0$ K at $p_c = 0.190 \pm 0.011$ (black dashed line). Note that the value of T_c is a function not only of p but also of disorder[24,27], possibly leading to systematic differences in carrier concentration estimates. Furthermore, the $T_c(p)$ relationships for Hg1201 and YBCO differ below optimal doping, and the systematic deviation from a parabolic form might result from a tendency towards stripe-order formation near $p = 1/8$ (ref. 27). In the inset, p for Hg1201 is estimated using the $T_c(p)$ relationship for YBCO[27], and linear extrapolation gives $p_c = 0.194 \pm 0.025$ (Hg1201) and $p_c = 0.196 \pm 0.011$ (YBCO). Symbols are plotted with area proportional to signal intensity estimated at $T = 0$ K. Samples at relatively high doping did not show an observable magnetic signal (see also Supplementary Fig. 1 for YBCO). Error bars represent the uncertainty in the estimation of T_{mag}. The results are summarized in Table 1. For the most underdoped Hg1201 sample B′, an order parameter fit was attempted, allowing for a small distribution of transition temperatures T_{mag}. This distribution was estimated from the superconducting transition width and the approximate change of T_{mag} with T_c. Fits to the (100) and (101) Bragg peaks were carried out to extract T_{mag} and the exponent β; β was found to be strongly dependent on the range of the fit, which was unstable for $T > 300$ K, and yielded $\beta = 0.18 \pm 0.13$ for $T > 250$ K and $\beta = 0.42 \pm 0.12$ for $T > 200$ K.

Table 1 | Summary of results for the universal pseudogap phase diagram

P	T_c (K)	T_{mag} (K)	I_{mag} (mb)
Y 0.091	54	300 ± 10	2.8 ± 0.3
Hg 0.069 (0.102)	61	372 ± 13	4.2 ± 0.3
Y 0.107	61	250 ± 20	1.7 ± 0.2
Y 0.112	63	235 ± 15	1.6 ± 0.2
Y 0.115	64	220 ± 20	1.5 ± 0.2
Y 0.135	78	170 ± 30	0.6 ± 0.1
Hg 0.105 (0.134)	79	248 ± 23	0.5 ± 0.1
Hg 0.107 (0.136)	81	228 ± 18	0.6 ± 0.1
Hg 0.116 (0.144)	89	N/A	<0.15
Y 0.147	89	N/A	<0.2
Y 0.209	75	N/A	<0.1

The hole concentration p estimated from the $T_c(p)$ relationships reported previously[27,28] (values for Hg1201 in parentheses are those pertaining to the inset to Fig. 3), superconducting transition temperature, onset temperature and strength of magnetic signal reported in this work and in[14,15]. Hg and Y denote Hg1201 and YBCO, respectively. The data are shown in Fig. 3. Neutron diffraction data for the YBCO 0.147 sample can be found in Supplementary Fig. 1.

(**P** in the scattering plane). These observations are further supported by the data in Fig. 2g, which demonstrate that the magnetic signal is even stronger at $\mathbf{Q} = (100)$ than at (101), whereas at the (201) and (102) reflections no signal was discerned. This trend, which is in good agreement with the results for YBCO[14], is consistent with the general expectation that magnetic signal decreases with increasing Q. However, the sharp decrease of the intensity with increasing Q implies that, distinct from conventional spin order, the magnetic density has a large spatial extent, consistent with a picture of extended spontaneous orbital currents within the unit cell. Moreover, the currents cannot be confined to the CuO_2 planes (Fig. 1g), as this would not lead to a strong L-dependence. Very recent theoretical work on extended two-dimensional Hubbard models including apical oxygen orbitals supports this picture[22].

The maximum T_c occurs close to where the experiment fails to discern a magnetic signal, and it seems likely that the order competes with the superconductivity. One intriguing possibility is that the fluctuations associated with an underlying quantum critical point are directly responsible for the appearance of superconductivity and the unusual normal state properties, such as the linear resistivity found up to remarkably high temperatures.

Received 14 May; accepted 2 July 2008.

1. Timusk, T. & Statt, B. The pseudogap in high-temperature superconductors: an experimental survey. *Rep. Prog. Phys.* **62,** 61–122 (1999).
2. Norman, M. R., Pines, D. & Kallin, C. The pseudogap: friend or foe of high T_c? *Adv. Phys.* **54,** 715–733 (2005).
3. Laughlin, R. B. A critique of two metals. *Adv. Phys.* **47,** 943–958 (1998).
4. Sachdev, S. Quantum criticality: competing ground states in low dimensions. *Science* **288,** 475–480 (2000).
5. Tallon, J. L. & Loram, J. W. The doping dependence of T^*: what is the real high-T_c phase diagram? *Physica C* **349,** 53–68 (2001).
6. Lee, S.-H. *et al.* Search for orbital moments in underdoped cuprate metals. *Phys. Rev. B* **60,** 10405–10417 (1999).
7. Stock, C. *et al.* Neutron scattering search for static magnetism in oxygen-ordered $YBa_2Cu_3O_{6.5}$. *Phys. Rev. B* **66,** 024505 (2002).
8. Sidis, Y. *et al.* Antiferromagnetic ordering in superconducting $YBa_2Cu_3O_{6.5}$. *Phys. Rev. Lett.* **86,** 4100–4103 (2001).
9. Mook, H. A. *et al.* Polarized neutron measurement of magnetic order in $YBa_2Cu_3O_{6.45}$. *Phys. Rev. B* **69,** 134509 (2004).
10. Sonier, J. E. *et al.* Anomalous weak magnetism in superconducting $YBa_2Cu_3O_{6+x}$. *Science* **292,** 1692–1695 (2001).
11. Sonier, J. E. *et al.* Correlations between charge ordering and local magnetic fields in overdoped $YBa_2Cu_3O_{6+x}$. *Phys. Rev. B* **66,** 134501 (2002).
12. Kaminski, A. *et al.* Spontaneous breaking of time-reversal symmetry in the pseudogap state of a high-T_c superconductor. *Nature* **416,** 610–613 (2002).
13. Borisenko, S. V. *et al.* Circular dichroism in angle-resolved photoemission spectra of under- and overdoped Pb-Bi2212. *Phys. Rev. Lett.* **92,** 207001 (2004).
14. Fauqué, B. *et al.* Magnetic order in the pseudogap phase of high-T_c superconductors. *Phys. Rev. Lett.* **96,** 197001 (2006).
15. Mook, H. A. *et al.* Observation of magnetic order in a YBa2Cu3O6.6 superconductor. *Phys. Rev. B* **78,** 020506 (2008).
16. Emery, V. J. & Kivelson, S. A. Importance of phase fluctuations in superconductors with small superfluid density. *Nature* **374,** 434–437 (1995).
17. Lee, P. A. Pseudogaps in underdoped cuprates. *Physica C* **317,** 194–204 (1999).
18. Anderson, P. W. *et al.* The physics behind high-temperature superconducting cuprates: the 'plain vanilla' version of RVB. *J. Phys. Cond. Mater.* **16,** R755–R769 (2004).
19. Varma, C. M. Non-Fermi-liquid states and pairing instability of a general model of copper oxide metals. *Phys. Rev. B* **55,** 14554–14580 (1997).
20. Varma, C. M. Theory of the pseudogap state of the cuprates. *Phys. Rev. B* **73,** 155113 (2006).
21. Chakravarty, S., Laughlin, R. B., Morr, D. K. & Nayak, C. Hidden order in the cuprates. *Phys. Rev. B* **63,** 094503 (2001).
22. Weber, C., Läuchli, A., Mila, F. & Giamarchi, T. Orbital currents in extended Hubbard models of high-T_c cuprates. Preprint available at ⟨http://arxiv.org/abs/0803.3983⟩.
23. Putilin, S. N., Antipov, E. V., Chmaissem, O. & Marezio, M. Superconductivity at 94 K in $HgBa_2CuO_{4+\delta}$. *Nature* **362,** 226–228 (1993).
24. Eisaki, H. *et al.* Effect of chemical inhomogeneity in bismuth-based copper oxide superconductors. *Phys. Rev. B* **69,** 064512 (2004).
25. Bobroff, J. *et al.* ^{17}O NMR evidence for a pseudogap in the monolayer $HgBa_2CuO_{4+\delta}$. *Phys. Rev. Lett.* **78,** 3757–3760 (1997).
26. Zhao, X. *et al.* Crystal growth and characterization of the model high-temperature superconductor $HgBa_2CuO_{4+\delta}$. *Adv. Mater.* **18,** 3243–3247 (2006).
27. Liang, R., Bonn, D. A. & Hardy, W. N. Evaluation of CuO_2 plane hole doping in $YBa_2Cu_3O_{6+x}$ single crystals. *Phys. Rev. B* **73,** 180505 (2006).
28. Yamamoto, A. *et al.* Thermoelectric power and resistivity of $HgBa_2CuO_{4+\delta}$ over a wide doping range. *Phys. Rev. B* **63,** 024504 (2001).
29. Xia, J. *et al.* Polar Kerr-effect measurement of the high-temperature $YBa_2Cu_3O_{6+x}$ superconductor: evidence for broken symmetry near the pseudogap temperature. *Phys. Rev. Lett.* **100,** 127002 (2008).
30. Aji, V. & Varma, C. M. Spin order accompanying loop-current order in cuprate superconductors. *Phys. Rev. B* **75,** 224511 (2007).

Supplementary Information is linked to the online version of the paper at www.nature.com/nature.

Acknowledgements We thank H. Alloul and C. Varma for comments. The work at Stanford University was supported by grants from the US Department of Energy and the National Science Foundation.

Author Information Reprints and permissions information is available at www.nature.com/reprints. Correspondence and requests for materials should be addressed to M.G. (greven@stanford.edu).